CDDpress

www.nature.com/cddiscovery

ARTICLE OPEN

Reformed islets: a long-term primary cell platform for exploring mouse and human islet biology

N. Haq[1,3], K. W. Toczyska[1,3], M. E. Wilson[1], M. Jacobs[1], Min Zhao[1], Y. Lei[1], Z. Shen[1], J. A. Pearson[2], S. J. Persaud[1], T. J. Pullen[1] and G. A. Bewick[1]✉

Pancreatic islets are 3D micro-organs that maintain β-cell functionality through cell–cell and cell-matrix communication. While primary islets, the gold standard for in vitro models, have a short culture life of approximately 1–2 weeks, we developed a novel protocol that employs reformed islets following dispersion coupled with a fine-tuned culture environment. Reformed islets exhibit physiological characteristics similar to primary islets, enabling high-resolution imaging and repeated functional assessment. Unlike other in vitro platforms, reformed islets retain an immune population, allowing the study of interactions between β cells and resident and infiltrating immune cells. Analyses showed that reformed islets have a similar composition and cytoarchitecture to primary islets, including macrophages and T cells, and can secrete insulin in response to glucose. Reformed islets exhibited partial dedifferentiation compared to native islets but were otherwise transcriptionally similar. The reformed islets offer a useful platform for studying diabetes pathology and can recapitulate both T1DM and T2DM disease milieus, providing an advantage over other models, such as mouse and human β-cell lines, which lack the input of non-β-endocrine cells and immune cell crosstalk.

Cell Death Discovery (2024)10:480 ; https://doi.org/10.1038/s41420-024-02234-6

INTRODUCTION

The prevalence of both type 1 and type 2 diabetes mellitus (T1DM, T2DM), which are among the leading causes of morbidity and mortality, is rapidly increasing, making it one of the largest global health concerns, affecting 537 million adults worldwide [1–3]. Although effective treatments exist for T2DM, intensive insulin therapy and islet transplantation for a limited number of people are the only approved option for T1DM despite improvements in care. For both types, treatment aims to manage symptoms and reduce complications; however, there is no cure.

Diabetes pathogenesis involves a complex interplay of multiple mechanisms, including genetics, islet/β-cell dysfunction, and immune dysregulation. As such, efforts to understand disease pathology have focused on comprehensively exploring and understanding all aspects of islet biology. Islets are micro-organs that regulate glucose homoeostasis through the secretion of the key hormones insulin, glucagon, and somatostatin. They comprise interspersed β, α, δ, ε, and PP cells intermingled with resident immune cells, stellate cells, smooth muscles, and fibroblasts [4]. β-cell functionality is maintained via cell–cell and cell-matrix communication. Therefore, understanding islet physiology and pathological dysfunction requires exquisite knowledge of how all islet cells communicate to maintain normal function, and how this is dysregulated to drive disease progression.

Primary islets, often isolated from rodents, are the gold standard for diabetes research. They are readily available and cost-effective, and their function is comparable to those observed in vivo [5]. However, isolating pancreatic islets requires significant time and effort, and limited experiments can be performed because of their short culture life, usually no more than a week before significant reductions in functionality are evident [6]. This is equally true for primary human islets which are available for research purposes from islet transplantation programmes. These limitations have restricted investigations, such as high-resolution live imaging of islets over prolonged periods or repeated functional assessments, owing to the short culture life and insufficient techniques for culturing adherent primary islets. Other alternatives, such as β-cell lines, including MIN6 cells (mouse), EndoC-β-H1 (human) or EndoC-β-H5 (human), can be cultured on glass, but they are transformed β-cell lines and therefore lack the signalling input of non-β cells, including other hormone-producing cells and immune cells [7]. Although two-dimensional culture of dispersed islet cells is possible on plastic surfaces, it requires a coating with cell-derived extracellular matrices. This includes extracellular matrix secreted from human carcinoma cells or bovine corneal epithelial cell matrix, which have high batch-to-batch variability and are linked to β-cell dedifferentiation [8–10].

In recent years, 3D culture of organ-like structures has paved the way for understanding the pathology of various diseases, aided drug discovery, enabled the identification of novel therapeutic targets, and enhanced personalised medicine. Therefore, developing novel 3D models of pancreatic islets is of high importance to aid the study of the pathophysiology of diabetes and to better understand the response to various compounds and therapeutics. Dispersion of whole islets and their subsequent

[1]Department of Diabetes, School of Cardiovascular and Metabolic Medicine & Sciences, Diabetes Endocrinology and Obesity Clinical Academic Partnership, King's College London and King's Health Partners, Guy's Campus, London, UK. [2]Diabetes Research Group, Division of Infection and Immunity, School of Medicine, Cardiff University, Cardiff, UK. [3]These authors contributed equally: N. Haq, K. W. Toczyska. ✉email: gavin.bewick@kcl.ac.uk

Received: 20 December 2023 Revised: 19 October 2024 Accepted: 30 October 2024
Published online: 23 November 2024

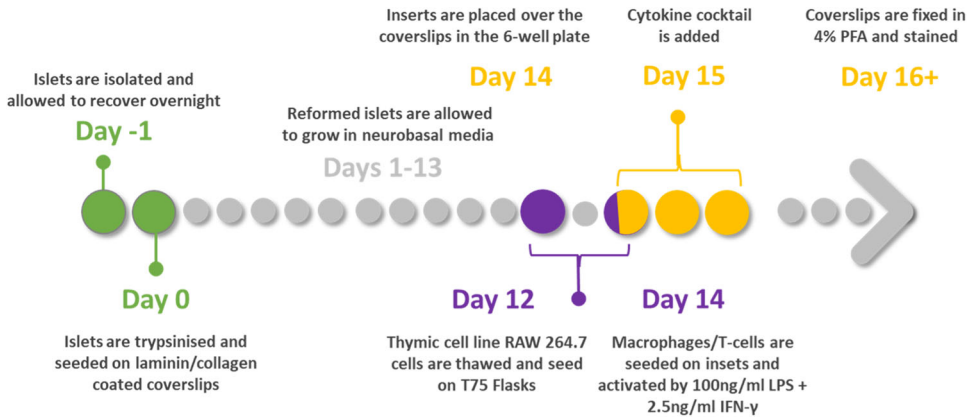

Fig. 1 Overview of reformed protocol. Native islets isolated from mouse or human donors were allowed to recover overnight. On day 0 they were trypsinised and seeded at a density of 35,000 cells/cm^2 on laminin-coated or collagenase-coated glass coverslips. They required 3–4 days of culture to adhere and spread on the glass surfaces, and 10–14 days to form reformed islets. Experiments were performed thereafter.

Table 1. Comparison of the sizes and composition of mouse and human native and reformed islets.

Charecteristics	Mouse native islets	Mouse reformed islets	Human native islets	Human reformed islets
Size	192.8 ± 13.54	173.7 ± 19.11	126.3 ± 18.71	181.1 ± 20.7
Beta cells	76.53 ± 2.96	72.64 ± 3.28	65.79 ± 9.16	66.38 ± 6.39
Alpha cells	9.08 ± 1.78	4.86 ± 0.77	26.56 ± 2.21	26.73 ± 1.52
Delta cells	11.75 ± 1.77	6.02 ± 0.97	12.31 ± 4.16	9.225 ± 1.25

reaggregation into spheroids offers one such method with the advantage of adherent long-term culture under suitable conditions and the potential for more efficient transgene delivery. A previous study attempted to use reaggregation and the subsequent formation and maintenance of islet organoids by using novel expansion and proliferation culture media. These islet clusters harboured key islet hormone-producing cell types and showed a higher degree of proliferation than native islets. However, this paradigm has limitations such as: (i) islet-derived cell clusters could only be generated from pregnant mice or wild-type rats, (ii) cluster numbers were small and inadequate for transcriptomic studies, (iii) the islet clusters were not functionally evaluated, and (iv) the presence of a resident immune population was not determined [11]. Stem cell-derived pancreatic organoids are an alternative. These cells are generated by directed differentiation of pluripotent stem cells and can be cultured over the long term. However, they also suffer from limitations, including not exhibiting all hormone-producing cell types, non-physiological insulin secretion, and a lack of a resident immune population.

Given the need for alternative methods for the long-term culture of primary islets, we aimed to refine reaggregation techniques to generate a superior adherent 3D islet culture platform using native murine or human islets as the source. These reaggregated islets are referred to as reformed islets. They can be maintained in culture for at least 4–6 weeks (Fig. S1), making them ideal for long-term studies, including high-resolution imaging, suitable for repeated functional assessment, and studying cell–cell communication. We found the reformed islets to be architecturally, transcriptionally, and functionally highly similar to the native islets they are generated from.

RESULTS

Reformed islets present organotypic cytoarchitecture akin to native primary islets

We optimised the reaggregation of islet cells by integrating a previously published protocol [10] with several enhancements and a more extensive validation process. The critical modification involved extending the maturation time after cell disaggregation and seeding from 4 days to 14 (Fig. 1). This extended period enabled the cells to re-aggregate and develop into 3D spherical structures, whereas they remained as a monolayer using the previous protocol. Furthermore, once the reformed islets reached maturity, they were successfully maintained on the platform for 42 days. This extended culture time allowed us to observe the long-term viability and functionality of the reformed islets.

After seeding, single islet cells adhered to the coated coverslip, and within several days, these cells formed a nonconfluent but connected network. After seven days of culture, focal points within the network began to form 3-dimensional spheroid structures (Fig. S2A) that harboured multi-hormonal cells producing insulin, glucagon, and somatostatin (Fig. S2B). Interestingly, multi-hormonal cells are also observed in developing foetal pancreas, the majority of which with age, become mono-hormonal [12]. At 14–16 days, spheroids were fully formed and exhibited a native islet-like cytoarchitecture with distinct hormone-producing populations. As the spheroid structures grew, we observed fibroblasts around the reformed islets. Once the reformed islets attained their maximal size, the fibroblasts regressed, forming space in between the reformed islets and the fibroblasts (Fig. S1A). The size of the reformed mouse islets was comparable to that of the native mouse islets, whereas human reformed islets tended to be slightly larger than their native counterparts (181.1 ± 2.07 vs 126.3 ± 18.71) (Table 1) (Fig. 2C, G). Typically, with 35,000 seeded islet cells, 14.50 ± 6.17 reformed mouse islets and 10.29 ± 2.93 reformed human islets were obtained per cover slip (Fig. 2P). We predict the reformed islets could be sized down to fit 96 well plates or sized up as required. For example, for 96-well plate, 15,000 islet cells could be seeded.

We evaluated the cellular composition of mouse-reformed islets at day 14 and day 42. On day 14, the β cells comprised 72.64%, α cells 28.06%, δ cells 6.02% whilst the resident immune population constituted 3.89% of the total cell population (Fig. 2D). On day 42, cellular composition was 79.46% β cells, 18.02% α cells, 7.52% δ cells and 1.58% for the immune population (Fig. S6A–E).

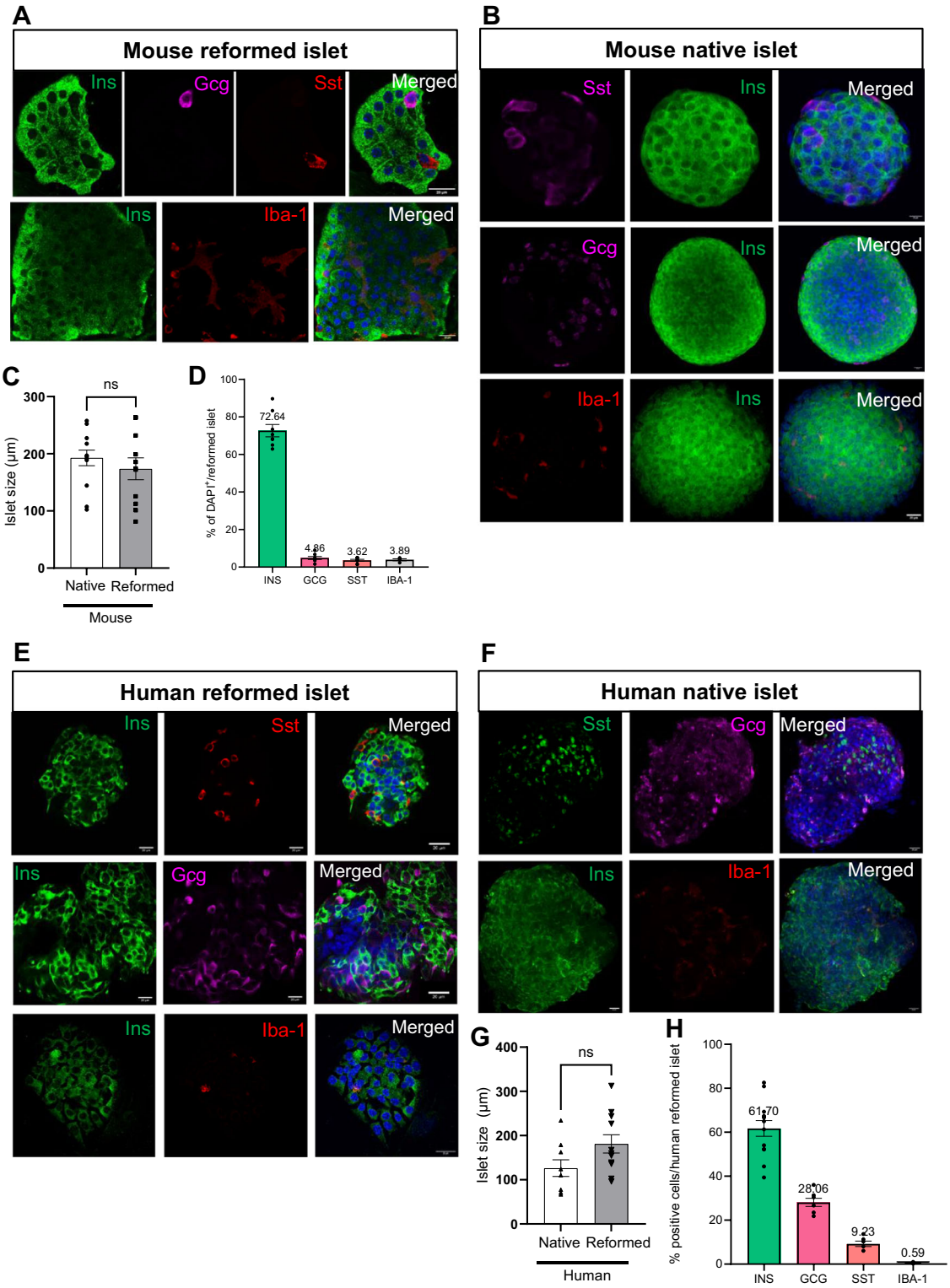

Fig. 2 Comparative and quantitative analyses of size, number, and cell composition of native and reformed islets at day 14. The native and reformed islets were immunolabelled for insulin, glucagon, somatostatin and inflammation marker IBA, and analysed using the cell counter plugin in ImageJ software. Mature mouse and human reformed islets (**A**, **E**) and mouse and human native islets (**B**, **F**) were immunoprobed with antibodies against insulin (INS; green), glucagon (GCG; purple), somatostatin (SST; red) and (Iba-1; red). DAPI nuclear staining is shown in blue. Scale bar is 20 µm. Sizes of native and reformed mouse (**C**) and human (**G**) islets were compared and presented in Table 1. Percentages of different cell types in mature mouse (**D**) and human (**H**) reformed islets were calculated and compared to native islets (mouse: **I**–**L**, human: **M**–**O**). These were based on calculation as a percentage of all DAPI-positive cells per reformed islet. (**P** represents the number of mouse and human reformed islets obtained with seeding of 35,000 islet cells. Numerical data are presented as the mean ± SEM, $n = 6$–13 observations (no. of islets per experiment) in 6–10 coverslips containing reformed islets. *ns* represents $p > 0.05$, unpaired Student *t*-test or One-way ANOVA, Dunnett's multiple comparisons test.

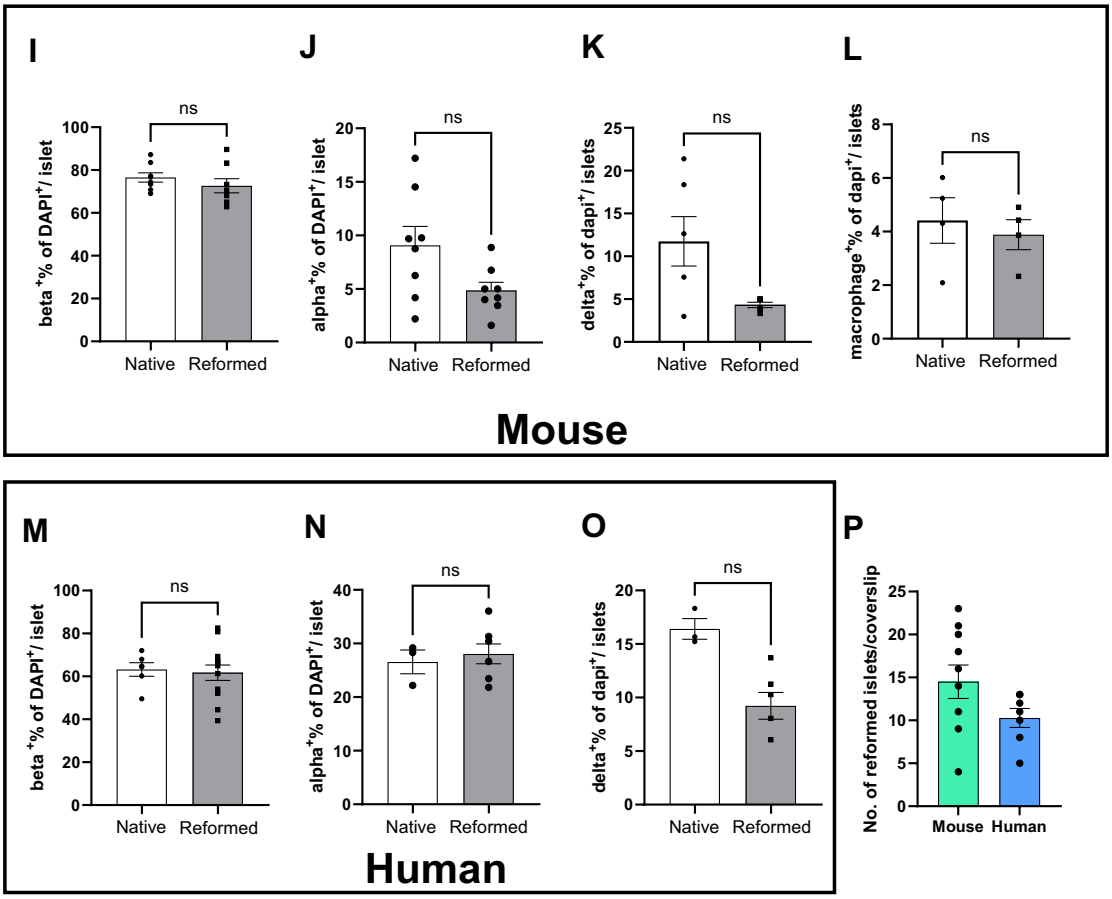

Fig. 2 (Continued)

Next, we compared the cellular composition of the major cell types between native and reformed islets in both mouse and humans. In mouse, the percentages of *β-* (p *val* = 0.48), α-cell types (*p-val* = 0.41) and macrophage cells (*p-val* = 0.51) were similar to those of reformed islets. The percentage of δ cells was slightly lower ($p = 0.1$) (Fig. 2I–L). Notably, the distribution of glucagon-positive cells in the reformed islets was similar to that observed in the native islets being localised predominantly in the periphery (Fig. 2B, D).

Similarly, in human reformed islets, the cellular arrangement and composition (β-61.70%, α-28.06%, δ-9.23%) closely resembled that of native human islets which contain 50–60% β cells, 30–50% α cells and 9–10% δ cells (Fig. 2H). In human native and reformed islets, the percentages of β cells ($p = 0.98$) and α cells ($p = 0.99$) were similar. However, we also found a lower percentage of δ cells in the reformed human islets as we did for mouse islets ($p = 0.59$) (Fig. 2M–O). The distribution of human glucagon-positive and somatostatin-positive cells mirrored that of native human islets, where they were interspersed with β cells (Fig. 2E, F). The hormonal cell composition and positional pattern in both mouse and human reformed islets support the notion that our modified platform is an excellent mimic of primary native islets.

In addition to hormone-producing cell types, a resident immune population is present in both murine and human islets [13]. This immune population is key to normal function and accounts for approximately 2–3% of all islet cells. Macrophages (MΦ) and dendritic cells (DC) are the predominant fraction in both mouse and human islets, but other immune cell types, such as CD4 and CD8 T cells are also present (Figs. S3A–C and 2A, E, F (lower panel). Increasing evidence suggests that these immune cells play crucial roles in maintaining islet homoeostasis, fine-tuning islet development, and modulating insulin secretion [12, 14, 15]. Moreover, the resident immune population has been shown to contribute to the initiation and progression of diabetes. For instance, the resident macrophage population is believed to be one of the key initiators of islet T cell infiltration, a hallmark of T1DM. Immunolabelling of the reformed islets revealed the presence of both resident macrophages (identified by positivity for Iba-1, which is an ionised calcium-binding adaptor molecule 1) and resident T cells (identified by CD8 and CD4 immunoreactivity) (Fig. 2A, B, E, F (lower panel) and S3A–C). The presence of a resident immune population is an important advantage of our platform because all other long-term culture paradigms lack these cell types. Additionally, the immune population in the reformed islets was verified by quantitative PCR. Transcriptionally markers of the immune population, CD45 (*Ptprc*- marker of all immune cells) (Fig. S3D) and macrophages (*Adgre1*) (Fig. S3E), were comparable between native and reformed islets. Based on phenotype, macrophages can be divided into pro-inflammatory 'M1' and anti-inflammatory 'M2' macrophages, although this framework is acknowledged as being useful but simplistic [16]. Expression of the M1 (*Ccl2*, *Il*β*3*) and M2 (*Igf1*) [17, 18] markers of polarity (Fig. S3F, G) were comparable between reformed and native islets. Whereas expression of *Ccl25 and Arg1* (other M2 markers) were reduced (10%) in reformed islets.

Reformed islets are able to proliferate when exposed to a GLP-1 receptor agonist

Mature β cells within primary islets typically remain in a quiescent state. However, one potential approach to increase functional β cell mass to treat insulin-independent diabetes is to induce proliferation of the residual β-cell population. We

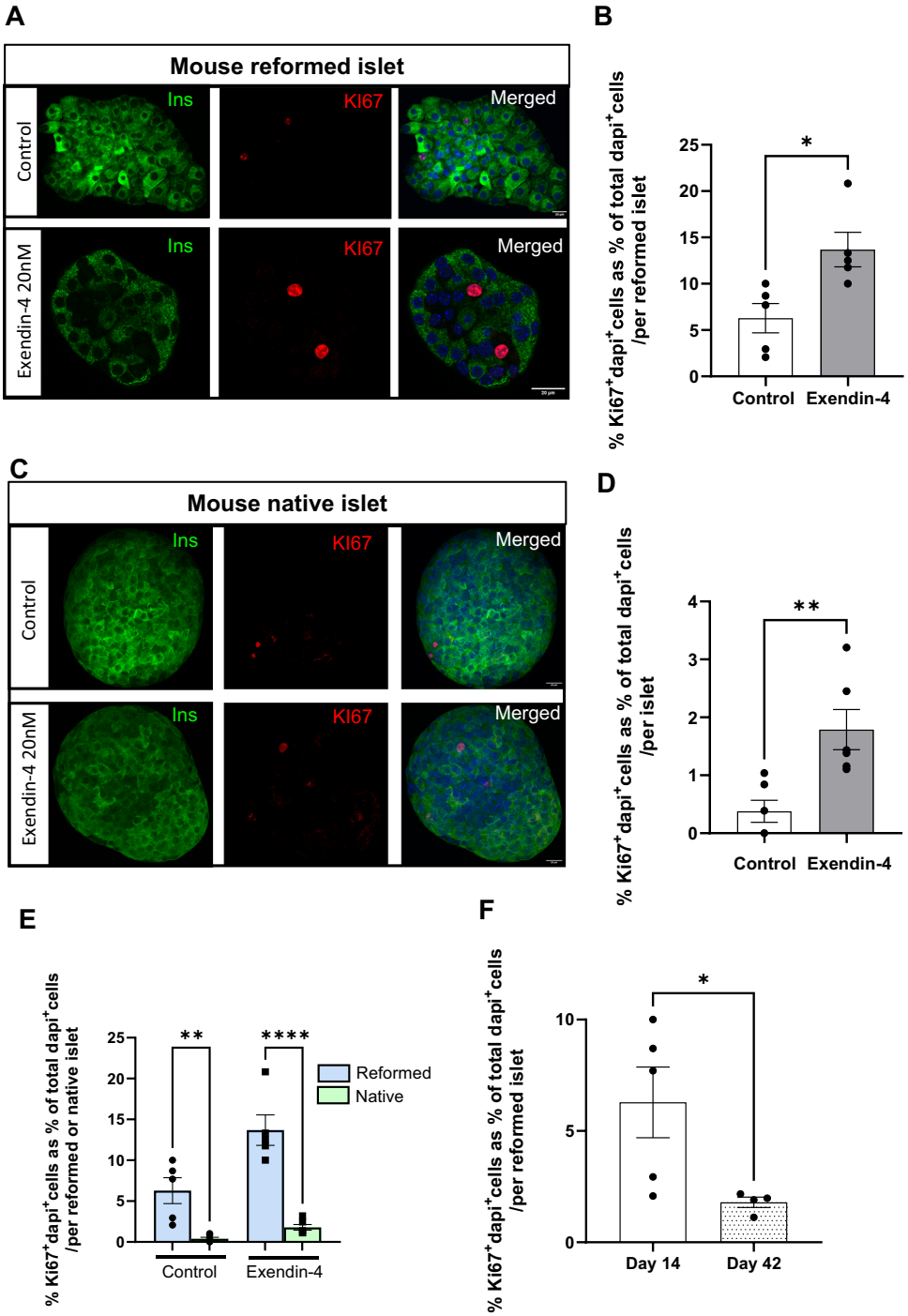

Fig. 3 Effects of exendin-4 on proliferation of mouse reformed islets. The reformed (**A**) and native islets (**C**) were exposed to exendin-4 for 30 h and immunoprobed with antibodies against insulin (INS; green) and Ki67 (red). DAPI is shown in blue in merged images. Scale bar is 20 µm. Percentage calculation of $Ki67^{+}DAPI^{+}$ cells within the reformed islets and native islets were performed using the cell counter plugin in ImageJ software (**B**, **D**, **E**). Data are expressed as mean ± SEM, $n = 5$ observations (10–15 of islets per experiment) from two separate experiments. *$p < 0.05$ relative to the control samples, One-way ANOVA, Dunnett's multiple comparisons test.

investigated whether reformed islets retained the ability to proliferate when treated with the GLP-1 receptor agonist exendin-4, which is known to enhance β-cell proliferation [19]. Exposure to exendin-4 significantly increased islet Ki67 immunolabelling ($p < 0.05$), which is a marker of cell proliferation (Fig. 3A, B) compared to native islets (Fig. 3C, D) suggesting our platform is useful for measuring islet cell proliferative responses. Of note, we observe differences in basal proliferation between native and reformed islets, where reformed islets were more proliferative. This was most pronounced on day 14 (6.28%) but was much less in mature reformed islets on day 42 (1.8%).

Functional insulin secretion machinery in reformed islets

The dissociation of whole islets into single cells leads to the loss of cellular connections, which can cause dysregulated insulin secretion [20]. Insulin secretion in response to glucose in the islets of Langerhans is a tightly regulated process that involves

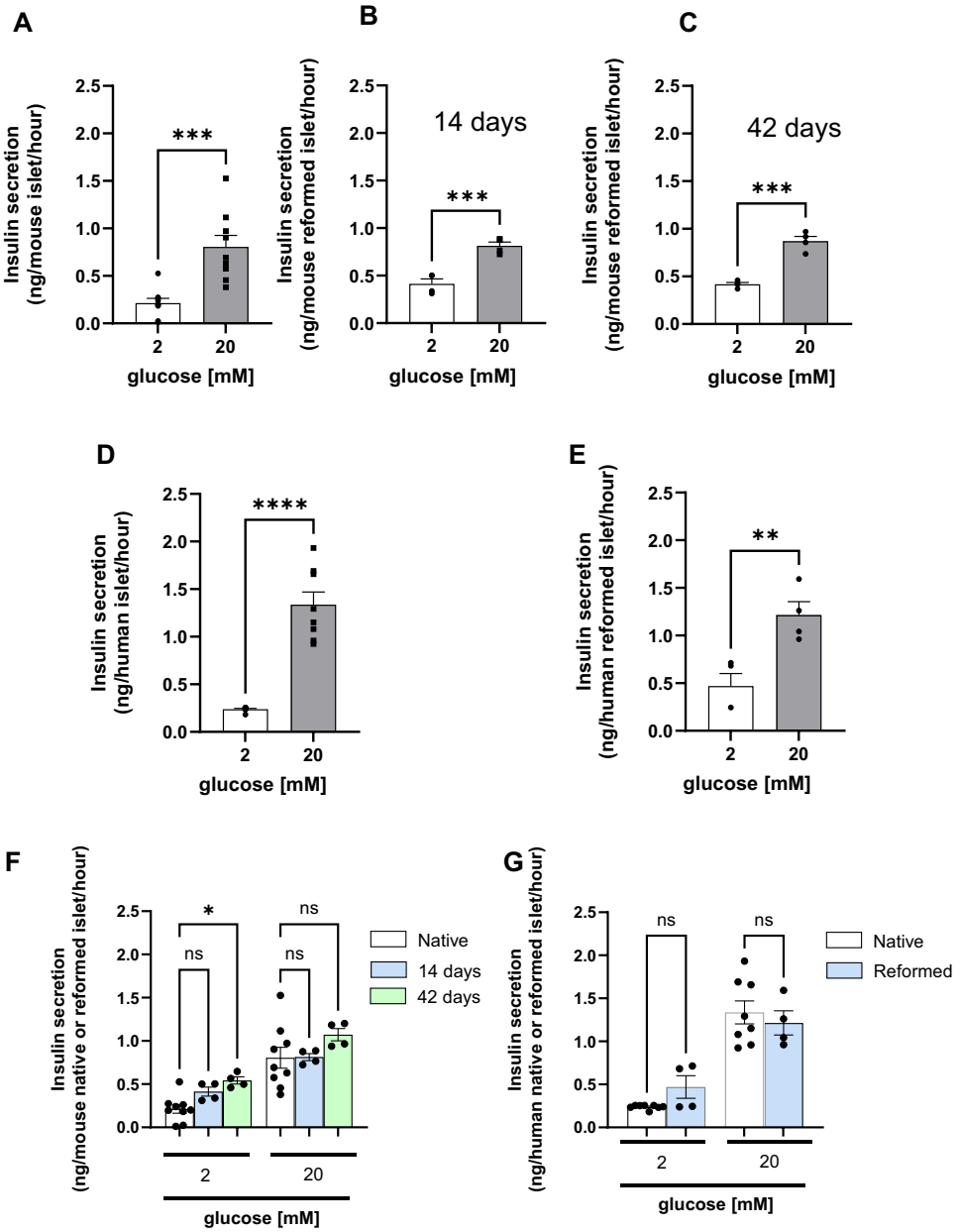

Fig. 4 Insulin secretory response of mouse and human reformed and native islets. Insulin secretion to supramaximal glucose concentration (20 mM) were assessed in primary islets (mouse—**A**, human—**D**) and reformed islets (mouse—**B**, **C**, human—**E**). In static incubation experiments, islets or reformed islets were pre-incubated for 2 h in Gey & Gey buffer supplemented with 2 mM glucose and then incubated for 1 h in the presence of either 2 mM or 20 mM glucose. Comparison between mouse native islets,14 days and 42 reformed islets were performed (**G**). Human native islets were compared with 14 days old human reformed islets (**H**). All data are shown as the mean ± SEM, $n = 4$–8 observations (representative of three experiments using mouse islets and human islets). *$p < 0.05$; **$p < 0.01$; ***$p < 0.001$; ****$p < 0.0001$ relative to the control samples at 2 mM glucose, unpaired Student *t*-test.

multiple cell types and signalling pathways. In response to glucose, mature primary islets display a biphasic insulin secretory response [21].

Insulin secretion was quantified in static incubation experiments using primary and reformed islets on both day 14 and day 42 of cultures. Acute exposure (1 h) to supramaximal glucose levels (20 mM) resulted in significantly increased levels of secreted insulin compared to 2 mM glucose (Fig. 4A–C, F) in both native and reformed mouse islets. Similarly, the concentrations of secreted insulin were comparable between the native and reformed human islets (Fig. 4D, E, G). This suggests that reformed islets are glucose sensing and capable of nutrient-driven insulin secretion.

Transcriptional analysis of reformed islets

Human pancreatic islets were obtained from a 36-year-old male cadaver with a BMI of 23 (>85% purity and >60% viability). More than 70% of raw reads were mapped to the reference genome. Globally, 1800 genes were differentially expressed with an adjusted p value < 0.05 when a cut-off value of >±2 was applied to the $\log_2$ fold change (FC) (Fig. 5A). Hierarchical clustering of the top 30 genes demonstrated significant differences between native and reformed islets (Fig. S4A). To further analyse these data, Kyoto Encyclopedia of Genes and Genomes (KEGG) enrichment analysis (Fig. 5B, C) was performed. Overexpression RNA-Seq analysis using significant $\log_2$FC discards a large proportion of the dataset that may be of biological relevance. Therefore, using the Molecular

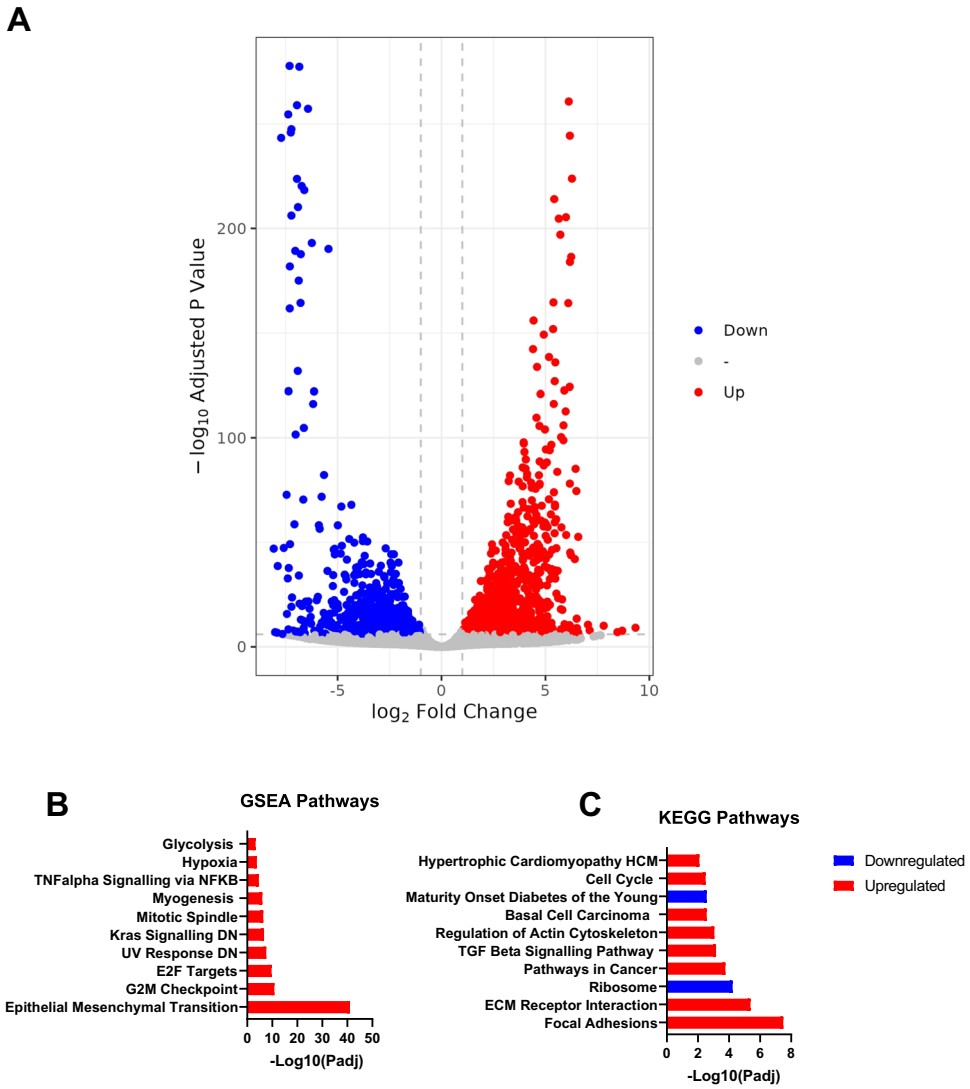

Fig. 5 Transcriptomic profiling of reformed human islets. A Volcano plot of all genes significantly upregulated or downregulated in reformed islets (log_2-fold-change >2, Benjamini–Hochberg corrected *p*-value threshold = 0.1). (**B** Gene set enrichment analysis (GSEA) of RNA-Seq data performed on reformed islets illustrates enriched pathways. **C** KEGG pathway analysis was performed for functional enrichment of genes in reformed islets.

Signature Database collection of hallmark genes, we performed Gene Set Enrichment Analysis (GSEA) [14, 22] on our dataset as a complementary method. The hallmark gene dataset is a compilation of various published well-defined biological processes or states that display coherent expression. GSEA uses only p-values, thereby reducing the variation and redundancy of gene expression across various pathways.

The enriched upregulated pathways included epithelial-mesenchymal transition (EMT) (*VACN, TGFB1, THBS2, LOXL2, ACTA2, ADAM12, SGCG, POSTN, COL1A1, CDH2,* etc.) (Fig. S4B), focal adhesion (*COL5A, PDGFRA, THBS2, COL1A2, FLNC, COL5A1, ITGA11, COL1A1, COMP*, etc.) (Fig. S4C), and skeletal system development (*PDGRFA, HAND2, HOXA1, HOXA3, HOXA4, HOXA5, SULF1, HOXC6, HOXC5, COL1A1*, etc.) (Fig. S4D). As expected, there were overlaps between genes with enriched pathways. The upregulation of transcripts encoding EMT genes, focal adhesions, and skeletal muscle development suggests that the EMT process is ongoing in cultured reformed islets. EMT has been found to be present in human epithelial cell cultures [23], and a recent study established that EMT occurs when human islets are allowed to expand in culture [24].

The downregulated differentially expressed genes (DEGs) were enriched in KEGG pathways related to ribosome biogenesis (*RPL11, RPL14, RPS6, RPL12, RPL21, RPL13, RPS15, RPS9, RPL3, RPS4X* etc.) (Fig. S4E), and Maturity Onset of Diabetes in the Young (MODY) (*NR5A, NKX6.1, GCK, INS, IAPP, ONECUT1, FOXAA3, FOXA2, HNF4A*, etc.) (Fig. S4F). Downregulation of ribosomal RNA (rRNA) transcription often occurs in response to intra- and extracellular stimuli in order to maintain homoeostasis. Downregulation of rRNA transcription has been associated with cellular processes such as cell cycle arrest and reduced cell growth, which may positively regulate cell differentiation [25]. Genes within the MODY pathway have been shown to be positively correlated with insulin secretion, and a decrease in gene expression has been associated with β cells being unable to maintain their mature phenotype [26, 27]. The expression of islet hormones, such as INS, GCG, SST, PYY, GHRL, and NPY, were generally mildly downregulated in reformed islets compared to their native source (Fig. S4G) despite the proportions of cell numbers being similar when assessed by immunostaining. Additionally, transcription factors related to the development of endocrine cells, such as RFX3, NKX6.1, FOXA2, and GLIS3, were downregulated (Fig. S4H). Collectively, the

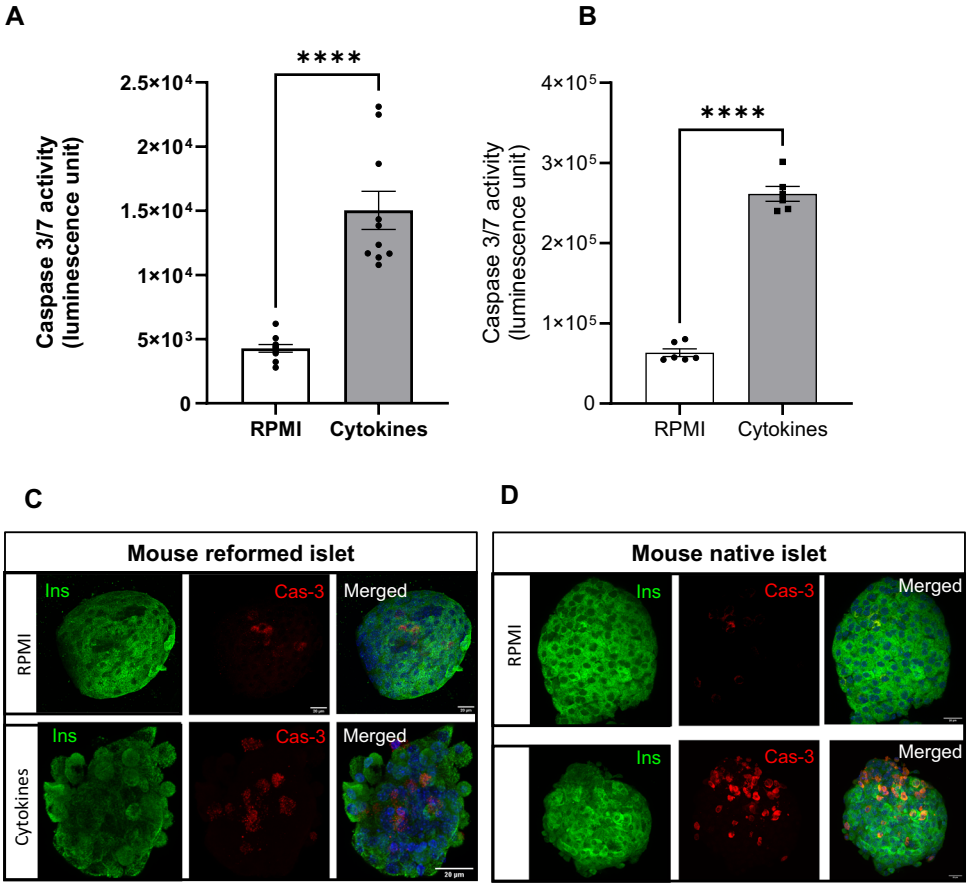

Fig. 6 The responses of mouse reformed islets to pro-inflammatory cytokines. Reformed and native islets were incubated with a mix of pro-inflammatory cytokines (IL-1β-, TNF-α, IFN-γ) for 24 h. Apoptosis of mouse reformed (**A**) and primary islets (**B**) was measured by quantifying caspase 3/7 activities using the Caspase-Glo 3/7 assay following a 24 h exposure to cytokines. In parallel, reformed and native islets were immunoprobed with antibodies against insulin (INS; green) and cleaved caspase 3 (CAS-3; red) (**C**, **D**). DAPI is shown in blue, and the scale bar is 20 µm. Data are shown as mean ± SEM; $n = 8$ observations (no. of islets per experiment) representative of three experiments. ****$p < 0.0001$ versus control; One-way ANOVA, Dunnett's multiple comparisons test.

transcriptional landscape of the reformed islets suggests that they have a high degree of similarity to the primary islets they are derived from but exhibit a partially dedifferentiated and relatively immature state. These features may aid long-term culture stability.

Reformed islets response to cytokine-induced damage mimics that of primary islets

Inflammatory responses and the presence of cytokines secreted by immune and non-immune cell types are central to both types of diabetes [28, 29]. While T2DM is associated with insulin resistance and β-cell dysfunction, recent studies in mouse models have linked an increase in circulating inflammatory factors, such as chemokines and cytokines, to islet inflammation and insulitis [30]. This is mainly due to the increased number of intra-islet macrophages that secrete cytokines such as IL-1β. Three cytokines have been implicated in this process: IFN-γ, produced by $CD4^+$ and $CD8^+$ T cells, and TNF-α and IL-1β-, produced by islet-infiltrating dendritic cells and macrophages [31]. The presence of this 'cytokine storm' orchestrates inflammation of islets with subsequent β-cell death in T1DM, and enhancement of insulin resistance with impairment of glucose homoeostasis in T2DM.

We modelled this 'cytokine storm' by addition of a cocktail of pro-apoptotic cytokines (IL-1β-, TNF-α and IFN-γ), and quantified caspase 3/7 activation in our reformed islets. Our results illustrated that cytokine-induced damage in mouse reformed islets (Fig. 6A) closely resembled that observed in primary mouse islets (Fig. 6B). We further qualitatively evaluated this cytotoxic damage by immunolabelling untreated and cytokine-treated native and reformed islets stained with antibodies directed against insulin and cleaved caspase-3, a surrogate marker of apoptosis. We observed that the untreated mouse reformed islets mostly maintained a round shape with clearly defined margins, in contrast to the cytokine-treated reformed islets that exhibited a loss of architecture with increased granularity, indicating islet destruction (Fig. 6C, D).

Reformed islets are a qualitative and quantitative platform to study immune invasion and migration

The development of insulitis is a common feature in both T1DM and T2DM. Although their aetiologies differ, the invasion and accumulation of macrophages and T cells in the islets display a pro-inflammatory phenotype [32, 33] that is common to both inflammatory processes.

Using our reformed islets, we modeled immune migration and invasion in both types of diabetes by co-culturing them with either T cells or macrophages in the presence or absence of a cytokine cocktail to drive a pro-inflammatory environment (Fig. 7A).

Migration assay. In native islets with insulitis, $CD8^+$ cells are the most abundant invading cell type and are reactive against β-cell antigen-presenting cells in T1DM. To mimic in vivo infiltration by autoreactive CD8 cells in islets, a transwell migration assay was performed to detect the migratory ability of $CD8^+$ cells. Reformed

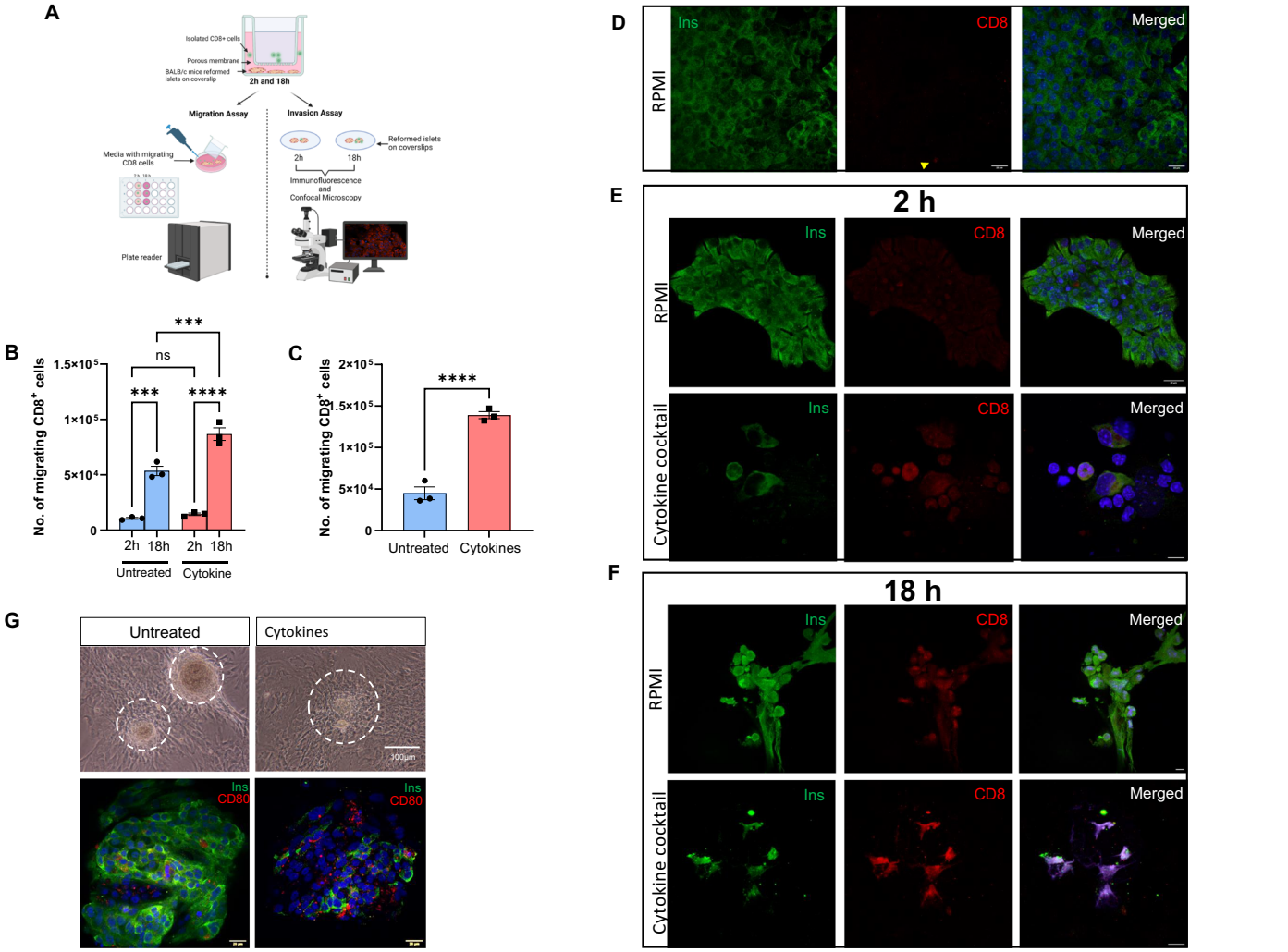

Fig. 7 Illustration of migration and invasion assays. Schematic diagram of ex vivo migration and invasion assays of $CD8^+$T cell and activated macrophages (RAW 264.7 cells) (**A**). Bar graph shows mean total percentage of $CD8^+$T cells migrating when cocultured with haplotype matched BALB/c reformed islets (**B**). Bar graph shows mean total percentage activated RAW 264.7 macrophage-like cells co-cultured with reformed CD1 mouse islets and number of migrating cells ± SEM for three independent migration experiments (**C**). Two-way ANOVA or unpaired Student *t*-test were performed to assess significance. ****p <0.0001. In invasion experiments, the reformed islets were immunolabelled with antibodies against insulin (Ins; green), CD8 (red) and a nuclear stain DAPI or investigated using light microscopy (**D**–**F**). Cytokine-induced destruction of reformed islets was investigated at time points 2 h (**E**) and 18 h (**F**) in comparison to non-cytokine treated (control; RPMI) reformed islets. The infiltration of reformed islets with RAW 264.7 macrophage cells were investigated in the presence of cytokines (**G**) and immunolabelled with insulin and CD80, a macrophage marker (Ins; green), CD80 (red) and counterstained with a nuclear stain DAPI.

islets were derived from BALB/c mice, and CD8 cells (haplotype matched) were harvested from the spleens of non-obese diabetic (NOD) mice, seeded onto the membrane of the transwell insert, and placed over coverslips with adherent reformed islets. As expected, haplotyped matched T cells migrated to reformed islets, and this process was significantly increased during inflammation. Additionally, we found significant increases in migratory T cells between untreated and cytokine-treated reformed islets at 18 h (Fig. 7B). To demonstrate the functional importance of the resident immune population in our platform, we depleted the resident macrophage population using clodronate liposomes. Treatment with clodronate liposomes significantly reduced expression of macrophages, as expected, and significantly decreased the migration of haplotyped matched T cells to reformed islets (Fig. S5A, B). This suggests the presence of resident macrophages plays a key role in calling toxic T cells to the islet, mimicking published in vitro data [17].

An increase in the number of islet-resident macrophages is prevalent in both types of diabetes [34, 35]. Specifically, T2DM is associated with meta-inflammation brought about by cytokines and chemokines released by macrophages. To model this, we co-cultured reformed islets with RAW264.7 cells a murine macrophage-like cell line. Under inflammatory conditions, RAW cell migration was significantly increased (Fig. 7C). This data further supports our platform for the study of islet immune responses in T2DM.

Invasion assay. Next, using qualitative confocal imaging we explored immune cell infiltration and destruction when exposed to external immune cells such as $CD8^+$ cells or macrophages. Reformed islets were co-cultured with T cells or activated RAW macrophage cells at baseline and during an inflammatory stimulus (cytokines). Invasion was imaged by immunostaining of immune cells (CD8 or CD80 antibodies) and β cells (insulin antibody) in combination with confocal microscopy. Reformed islets derived from BALB/c mice were co-cultured with $CD8^+$ T cells and qualitatively assessed at 2 and 18 h. After 2 h, we observed that reformed islets exposed to cytokines showed destruction of their

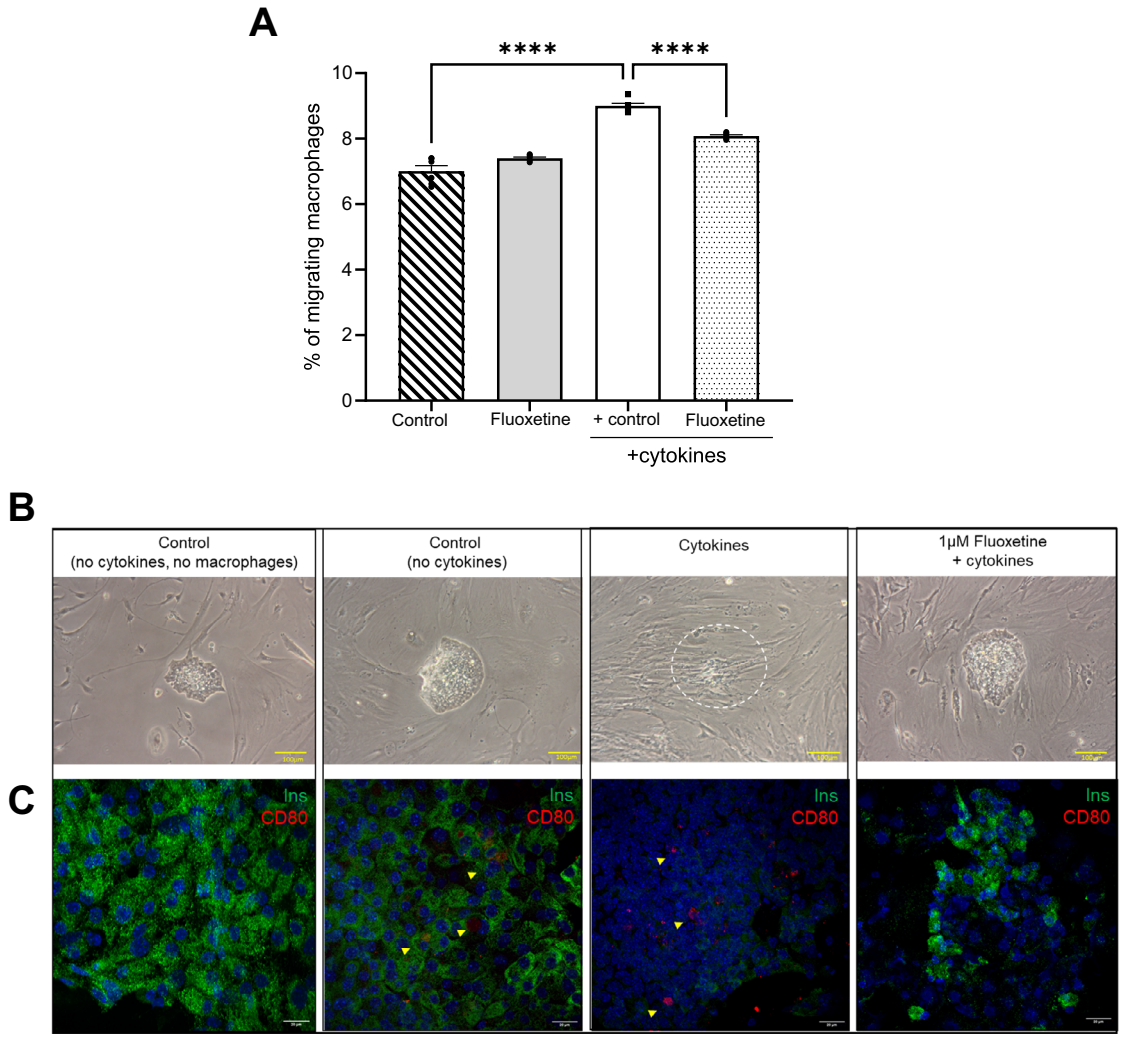

Fig. 8 Migration and invasion assay illustrating the effects of 1 μM fluoxetine, on reformed mouse islet infiltration by RAW 264.7 macrophage cells. The reformed islets were incubated with 1 μM fluoxetine for 48 h, and cytokines and LPS-activated macrophages were added during the last 24 h of culture. The migratory properties of RAW 264.7 cells were quantified by Cell Biolabs' CytoSelect™ cell migration and EZCell™ cell migration/chemotaxis assays (**A**). Reformed islets were fixed in 4% PFA prior to brightfield imaging and immunofluorescence (**B**, **C**). The reformed islets were visualised using light microscopy and immunoprobed with antibodies directed against insulin (green), CD80 (red), and DAPI was stained blue in parallel. Scale bars represent 100 μm for light microscopy and 20 μm for fluorescence microscopy. Data are expressed as mean ± SEM ($n = 3$ observations-no. of islets per experiment). ***$p < 0.0006$; ****$p < 0.001$ versus cytokine control, Two-way ANOVA, Dunnett's multiple comparisons test.

architecture and infiltration of $CD8^+$ cells compared with reformed islets not exposed to $CD8^+$ cells (Fig. 7D, E). After 18 h, both cytokine-treated and untreated reformed islets were completely invaded by $CD8^+$ cells, with complete destruction of the reformed islets (Fig. 7D, F). To exclude endogenous effect of the antibodies and autofluorescence, control staining with insulin and CD8 antibodies, primary antibodies only and secondary antibodies only, were labelled in reformed islets (Fig. S7).

To study macrophage invasion, reformed islets were exposed to an inflammatory stimulus and the invasive capability of LPS and IFN-γ activated RAW 264.7 cells was assessed. The number of infiltrating RAW 264.7 cells was qualitatively higher in the presence of cytokines than in untreated controls (Fig. 7G).

In summary, we have shown our reformed islet platform is effective at modelling various chemical and cellular immune insults and a key component of this is the presence of a functional resident immune population. Our platform is therefore an excellent system for identifying novel therapeutic interventions to prevent immune migration, infiltration and β-cell destruction.

Islet protective agent can cloak islets from immune cell infiltration. As proof of concept, we sought to validate the use of our platform to identify compounds that could prevent islet invasion and protect islets from damage. To this end, we assessed the islet-protective effects of fluoxetine. Fluoxetine is a commercially available anti-depressant drug that has been shown to significantly increase β-cell proliferation and protect islet cells from cytokine-induced apoptosis [13]. To replicate the protective effect of fluoxetine, reformed islets were exposed to a cytokine cocktail in the presence or absence of a therapeutic concentration of fluoxetine (1 μM) for 24 h while activated macrophages (RAW 264.7) were added to the inserts of the Transwell plate and cultured for a further 24 h. Quantitative analysis indicated a significant reduction in the number of migrating activated RAW cells when reformed islets were cultured under inflammatory conditions and treated with fluoxetine (Fig. 8A). Additional qualitative analysis by confocal microscopy illustrated the reduced migration and islet protection (Fig. 8B, C). Collectively, we show that reformed islets can be modelled to replicate the in vivo pathogenesis common to both T1DM and T2DM.

DISCUSSION

This study reports the development of a long-term biomimetic method to model native mouse and human islets ex vivo, while maintaining long-term islet functionality. We performed transcriptome profiling to evaluate how closely our model recapitulates native islets and glucose-stimulated insulin secretion, to assess functionality and evaluate islet morphology in terms of islet cell-type distribution and size. We further investigated the suitability of this platform for studying β-cell proliferation and immune cell-islet cell interactions by performing invasion and migration assays.

One of the major results of this study highlighted that reformed islets mimic primary islets and can survive for long periods in culture. In our protocol, disassociated primary islet cells are reaggregated and, over time, form 3D structures that mimic their primary counterparts.

This contrasts with previously reported protocols, in which reaggregated islet cells remain in a monolayer [9]. Both mouse and human reformed islets harbour the major islet hormone cell types arranged architecturally, and in proportions similar to primary islets [15, 36, 37]. The functionality of the reformed islets was assessed using insulin secretion on day 14 and 42 by β-cell proliferation, and cytokine-induced apoptosis assays. Our results indicate that glucose-stimulated insulin secretion is comparable to that observed in primary mouse and human islets [38]. In addition, we observed that reformed-islet cells could be stimulated to proliferate in the presence of exendin-4 and that cytokine-induced damage could easily be measured using a caspase 3/7 assay [39–41]. We observed the presence of fibroblasts surrounding the aggregated islet cells from day 4, which slowly regressed while reformed islets matured. The fibroblasts did not affect the functionality of the reformed islets, nor did they engulf the reformed islets. Interestingly, recent studies suggest that fibroblasts increase islet survival and function [42–44]. Our findings illustrate that reformed islets are an anatomical and functional alternative to native human and mouse islets, but which can be cultured for longer periods (4–6 weeks).

To understand how closely our reformed islets modelled native islets, we performed bulk RNA sequencing and transcriptomic analysis of freshly isolated native human islets and the reformed islets on day 16. Global expression profiling revealed a number of DEGs between native and reformed islets. However, functional clustering and pathway analyses of DEGs indicated an association with EMT hallmark genes in the reformed islets. These EMT-enriched genes have stem cell-like properties and may generate endocrine islets via committed precursor cells [32, 33]. It is plausible that dedifferentiation and reaggregation enable islets to withstand long-term culture conditions. Interpretation of our data should be cautious until it is corroborated by characterising reformed islets generated from additional donors. However, our study emphasises reformed islets can be derived from normoglycaemic patients and this platform may be widely utilised to study islet related pathology for downstream functional studies and omics' analysis.

One of the key advantages of our model is the presence of a resident immune population similar to that of native islets. Various studies have highlighted the role of resident immune cells, particularly macrophages, in islet development, β-cell homoeostasis, and regeneration, as well as in the pathology of diabetes [45, 46]. Indeed, the onset of diabetes, specifically T1DM, results from macrophage activation which drives the recruitment of $CD8^+$ and $CD4^+$ T cells to the islet, ultimately resulting in the destruction of β cells [47]. The lack of in vitro models where resident immune cells can be studied has hampered our understanding of this disease process. To our knowledge, this model is the first in which most immune cell types can be found.

Using reformed islets, we were able to recapitulate features of the immune infiltration observed in T1DM mechanisms by coculturing reformed islets generated from BALB/c mice and splenic $CD8^+$ T cells from haplotype-matched NOD mice. We speculate that this platform can be extended to human reformed islets by co-culturing haplotype-matched reformed human islets with human T-cell clones. Furthermore, we could also model T2DM. T2DM patients have an elevated number of macrophages infiltrating their islets [48, 49]. We modelled this phenotype by coculturing mouse reformed islets with macrophage-like RAW 264.7 and observed complete infiltration and destruction of islets in the presence of cytokines .

An important advantage of our platform is the presence of a functional resident immune population, which is absent in other models. Previous studies have demonstrated the critical role of MΦ in T1D pathology [50–54]. For example NOD mice do not develop insulitis or diabetes when resident MΦ are depleted [51, 55] and adoptive transfer of T cells isolated from these mice do not trigger diabetes [51, 52]. In our platform, depletion of clodronate sensitive immune cells, which includes macrophages, prevents toxic T-cell migration mirroring the published in vivo data. To our knowledge this is the first time the role of the resident immune population in immune migration to the islet has been modeled in vitro. Our platform offers a unique opportunity to further investigate the importance of the resident immune population.

Fluoxetine, an approved antidepressant drug has recently been shown to increase insulin secretion in response to glucose and to increase β-cell mass [13, 56, 57]. As a proof of concept, we chose this drug to validate our human reformed islet model, and qualitatively and quantitatively assess Fluoxetine's ability to protect islets against cytotoxic insults. As expected, the migration and invasion assays showed that fluoxetine reduced macrophage migration and inhibited islet apoptosis. Thus, our study demonstrated reformed islets can be used to identify new targets or could be employed as a screening platform to identify drugs which can protect β cells and prevent immune invasion, once optimised in a multi-well format [58].

Long-term imaging of pancreatic islets is challenging, and the gold standard method for measuring β-cell mass is to evaluate the pathological staining of fixed pancreatic tissue sections. However, this does not encompass the dynamic changes that the β-cell mass undergoes during the different stages of disease progression. Reformed islets allow a non-invasive, high-resolution system to quantitatively image at the single-islet level which can be useful for the evaluation of islet viability, proliferation, and the effects of novel anti-diabetic compounds. For example, reformed islets can be used to report macrophage infiltration by coculturing with transgenic-labelled fluorescent macrophages.

In summary, we have refined a method for generating a static reformed islet platform that can be applied to both mouse and human cells and cultured over a long period of time. Reformed islets are genotypically, phenotypically, and functionally like the primary islets they are derived from and importantly harbour a resident immune population, which is missing in other platforms. These properties make reformed islets highly amenable to exploring islet cell–cell communication, for example, using multiple imaging modalities and repeated functional assessment. The platform could easily be optimised for use in a multi-well format for high content screening programmes and will likely prove to be a relatively easy platform to genetically manipulate given the dispersion step in the methodology. Dispersed islets cells are far easier to transfect whether using lipid-based transfection reagents, viral vectors, or electroporation [59, 60]. We hope the platform will be a useful tool to further our understanding of diabetes pathology.

METHODS

Materials

Hanks' Balanced Salt Solution and Hepes buffer were obtained from Gibco, B27 (Thermo Fisher Scientific). Fluoxetine hydrochloride, collagenase type

XI, histopaque-1077, culture media, and supplements were purchased from Sigma-Aldrich. The primary antibodies used in this study are summarised in Supplementary Tables 1 and 2. Recombinant murine tumour necrosis factor α (TNF-α), interferon γ (IFNγ), and interleukin-1β (IL-1β) were purchased from PeproTech EC, and the Caspase-Glo 3/7 Assay Kit was purchased from Promega. $CD8^+$ cells were isolated from the spleens of four 8-week-old diabetic female NY8.3 NOD mice using a MojoSort Mouse CD8 T-cell isolation kit (Cat# 480043, BioLegend, San Diego, CA, USA) and MojoSort buffer (Cat# 480017, BioLegend). Cell Biolabs' CytoSelect™ cell migration assay from Cell Biolabs and EZCellTM cell migration/chemotaxis assay kits were purchased from BioVision. Clodronate liposomes (F70101C-AL-FOR-5ml) were purchase from Stractech Scientific Ltd.

Animal husbandry

CD-1 and BALB/c male mice were purchased from Charles River and were housed under temperature- (22 ± 2 °C) and light-controlled conditions (12 h light:12 h dark cycle) with ad libitum access to drinking water and a standard rodent chow diet. Splenocytes for CD8+ cell isolation was obtained from four 8-week-old female diabetic NY8.3 NOD mice (A kind gift from Dr. James Pearsons, Cardiff University). Animal experiments were performed in accordance with the British Home Office Animal Scientific Procedures Act (1986).

Human donors

Human islets were retrieved from non-diabetic, heart-beating, and brain-dead donors and isolated by cold collagenase digestion ([23, 61] with appropriate ethical approval from the King's College London Human Islet Research Tissue Bank (KCL HI-RTB; 20/SW/0074). Islets from two donors were used in this study. Donor 1 was 41 yr old female with a BMI of 24 and donor 2 was 36 yr old male with a BMI of 23.

Islet isolation

Mouse islets were isolated from male CD-1 mice (≥20 g) aged 8–12 weeks and separated from exocrine tissue by digestion with collagenase. Isolated mouse islets were cultured overnight (37 °C, 95%air/5%CO_2) in Roswell Park Memorial Institute (RPMI) 1640 Medium supplemented with 10% (v/v) foetal bovine serum (FBS), 100 U/ml penicillin and 100 µg/ml streptomycin, and 2 mM L-glutamine.

Preparation of matrix-coated coverslips

Round borosilicate glass coverslips (12 mm diameter and 0.17 mm thickness) were transferred to 24-well plates and coated with either laminin from Engelbreth-Holm-Swarm murine sarcoma basement membrane at 50 µg/ml or Collagen IV stock solution 1 mg/ml in Ca^{2+}/Mg^{2+}supplemented with Hanks Balanced Salt Solution (HBSS) overnight at 37 °C. The coverslips were washed in HBSS and left to dry for 10 min before seeding.

Preparation of reformed islets

Two thousand to two thousand and five hundred mouse or 1000 human islets were hand-picked from suspension cultures 24 h after isolation and washed with PBS. Islets were then dissociated into a suspension of single cells through trypsin digestion, which was stopped by adding neurobasal media consisting of MEM supplemented with 5% (v/v) FBS, 1× B-27, 1%(v/v) penicillin and streptomycin, HEPES 10 mM, Glutamax 1×, Na-pyruvate 1 mM, and 11 mM glucose. It is well known that FBS is widely used as a growth supplement, while optimal glucose concentration is vital for healthy cell growth. B-27 supplement is traditionally used to promote primary neuronal long-term survival and maturation in culture. Previous studies have shown that addition of B-27 to this media resulted in long-term highly viable islet cell cultures [9, 62]. Addition of Glutamax reduces toxic ammonia build up and also improves cell viability and growth. Last but not least HEPES maintains the pH stability of the media between the range of 7.2–7.6.

Islet cells were seeded at a density of 35,000 cells/cm^2 on laminin-coated or collagenase-coated glass coverslips. They required 3–4 days of culture to adhere and spread on the glass surfaces, and 10–14 days to form reformed islets. The culture media was replaced by neurobasal media every other day till they were ready for experiments. These reformed islets were used for all the experiments described here. In keeping consistent with widely established native islet study protocols, the culture media was changed to RPMI with 2% FBS with 1%(v/v) penicillin and streptomycin for all experiments.

Immunofluorescence and confocal microscopy

Immunofluorescence was used to study the cytoarchitecture of the reformed islets, as well as proliferation and cytokine-induced damage. Whole native islets or coverslips with 6–10 reformed islets were fixed with 4% PFA and incubated in blocking buffer (1%BSA + 10%donkey serum in 0.1% PBST) for 1 h at room temperature to eliminate non-specific antibody binding. Thereafter, the native or reformed islets were incubated with primary antibodies against insulin, glucagon, somatostatin, Ki67, CD80, IBA1, CD8, CD3e, and CD4 overnight at 4 °C and washed in PBS (Supplementary Table 1). The slides were subsequently exposed to appropriate secondary antibodies for 1 h at room temperature and washed with PBS (Supplementary Table 2). DAPI Fluoromount-G was used for the mounting. To demonstrate the specificity of the insulin and CD8 antibodies, primary and secondary antibody controls were performed to exclude endogenous reaction products (Fig. S7).

Images of the reformed islets were taken with an Eclipse Ti-E Inverted A1 confocal microscope or Zeiss LSM700 Confocal Microscope and analysed using CellProfiler, cell counter plugin in ImageJ software and IMARIS software.

Insulin secretion from mouse and human reformed islets

Insulin secretion from native and reformed mouse and human islets was measured by static incubation experiments. Reformed islets were pre-incubated for 1 h in physiological salt solution [63] supplemented with 2 mM glucose. Coverslips with 6–10 reformed islets were counted under a Nikon TMS phase-contrast microscope and incubated with appropriate volumes (100 µl of buffer per reformed islet) of Gey & Gey buffer supplemented with either 2 mM or 20 mM glucose. The supernatants were collected and stored at −20 °C prior to insulin radioimmunoassay.

Apoptosis: caspase-Glo 3/7 assay

Caspase-Glo 3/7 assay was used to detect apoptosis by measuring caspase 3/7 activity. Coverslips having 4–5 reformed islets and primary islets were exposed to a mix of pro-inflammatory cytokine cocktail (CK) (0.05 U/µl IL-1β-, 1U/µl TNF-α and 1U/µl IFN-γ) diluted in RPMI supplemented with 2% FBS and 1% Pen/strep for 24 h. Caspase 3/7 activity was quantified by bioluminescence according to the manufacturer's protocol.

Macrophage depletion in islets

Islets were cultured in liposomes containing either PBS or clodronate (600 µg/ml) (Stractech Scientific Ltd.) for 48 h. Islets were randomly handpicked for treatment.

Islet destruction: migration assay

The Transwell cell migration assay measures the chemotactic capability of cells toward a chemo-attractant. First, we isolated islets from CD1 mice, BALB/c mice, and human cadavers. BALB/c mice were used as they express the MHC class H2Kd haplotype and are therefore matched to antigen-specific T cells.

The reformed islets were incubated in RPMI supplemented with 2% FBS and 1% Pen/strep for 24 h. Subsequent studies using the selective serotonin reuptake inhibitor fluoxetine were chosen for migration and invasion studies, as there is evidence to support the anti-inflammatory and β-cell-protective properties of this drug [11, 13].

Simultaneously, RAW 264.7 cells were activated with LPS (200 ng/ml) and IFN-$_\Upsilon$ (2.5 ng/ml) for 24 h [64]. After washing with PBS to remove LPS and IFN-$_\Upsilon$, the RAW cells were trypsinised, pelleted, seeded (1×10^6 cells) into inserts (upper chamber), and placed over coverslips with at least 3–4 reformed islets for an additional 24 h.

$CD8^+$ cells were isolated from the spleens of four 8-week-old diabetic female NY8.3 NOD mice. Briefly, a single-cell suspension was prepared with MojoSort buffer at 1×10^8 cells/ml. Ten microliters of biotinylated antibody containing antibodies against CD4, CD11b, CD11c, CD19, CD24, CD45R/B220, CD49b, CD105, I-A/I-E, TER-119/Erythroid, and TCRγδ were added. The mixture was then incubated for 15 min on ice, and 10 µL streptavidin nanobeads were added. The final volume of 120 µL of the cell and bead mixture was incubated on ice for an additional 15 min. Finally, 120 µL was diluted in in 1× MojoSort buffer (2.5 mL) and placed in a MojoSort Magnet (Cat# 480019/480020, BioLegend) for 5 min for magnetic separation. The free cells in the solution were collected as enriched $CD8^+$ T cells.

The migration assay was measured using an 8 µm pore transwell plate (BioVision, Inc., USA) according to the manufacturer's protocol. Briefly, BALB/c reformed islets were incubated for 48 h in 2% FBS RPMI complete

medium in the lower chamber of a Transwell culture plate. Thereafter, 2×10^5 $CD8^+$ T cells were seeded into the upper chamber and placed over coverslips with reformed islets of both groups: untreated reformed islets and cytokine cocktail-exposed reformed islets. After 18 h of incubation, the cells in the lower chamber were quantified by measuring the O.D values at Ex/Em = 540/590 nm using a PHERAstar Microplate Reader.

To investigate reformed islets as a platform to perform migration studies, the effects of the drug fluoxetine on macrophage migration and reformed-islet destruction in the presence of pro-inflammatory cytokines were studied using established migration assay kits. Briefly, mouse or human reformed islets were incubated for 48 h in 2% FBS RPMI complete media with or without a drug of interest for the first 24 h. After the initial 24 h, activated monocyte/macrophage-like RAW 264.7, were seeded into the upper chamber (2×10^5 cells) and placed over coverslips with reformed islets. Pro-inflammatory cytokines were added for the final 24 h. After 24 h of incubation, the cells in the lower chamber were quantified by measuring the O.D values at Ex/Em = 540/590 nm using a PHERAstar Microplate Reader.

Islet destruction: invasion assay

A Transwell cell invasion assay was developed to measure both cell chemotaxis and invasion of islet cells through the extracellular matrix. This method is often used for studying cancer metastasis and embryonic development [65]. To this end, we studied the effects of cytokine-induced destruction of mouse and human reformed islets in the presence of $CD8^+$ cells and activated monocyte/macrophage-like cells RAW 264.7 and assessed by confocal imaging [66].

For this study, we used coverslips that underwent migration assays (described above). The coverslips were fixed and immunolabelled with insulin, CD8, or CD80 antibodies and counterstained with DAPI for the identification of nuclei. Qualitative analyses using light and confocal microscopy were used to assess the appearance of the reformed islets.

Bulk RNA-sequencing

Total RNA was extracted from three replicates (1000 islets per replicate) of native human islets and reformed islets from one donor, using the TRIzol method. Samples were uniquely barcoded and pooled into one sample. After sequencing, all the samples were distinguished based on their unique barcodes. The next step included In vitro Transcription, is a linear amplification step which results in amplified RNA (αRNA). This α-RNA was fragmented and run on an Agilent TapeStation to assess RNA integrity.

Reverse transcription, in addition to a PCR reaction, amplified the α RNA, and appropriate sequencing adaptors were added. During the PCR reaction, the material was again amplified, and appropriate adaptors for sequencing were added to the sequences. This resulted in a DNA library (cDNA) that could be used for sequencing. The cleaned cDNA library was run on an Agilent TapeStation instrument.

Library preparation and RNA sequencing were performed by Single-Cell Discoveries using the QuantSeq 3 kit (Lexogen) and sequenced on an Illumina NextSeq 500 with a sequencing depth of 10 million reads per sample. Raw sequencing data were aligned against the human reference genome using STARsolo (2.7.10a). Read quality checks were carried out using FastQC, after which BBDuk from the BBMap (version 38.87) software was used to trim Illumina adaptors and polyA tails. Reads were mapped to the hg38 reference human genome using Star Aligner.

Data processing

Bulk RNA-Seq analysis. The R package DESeq2 v1.36.0 [67, 68] was used to determine differential gene expression, and DEGs with padj <0.1 were selected. Variance-stabilising transformations of raw count data were used to visualise the sample clustering. All data were subjected to global-scale normalisation and log transformation. Linear dimensionality reduction was performed using principal component analysis on the top 500 genes from the variable-stabilising transformation dataset using the DESeq2 package. The data was also subject to shrinkage estimation of the $\log_2$ fold changes using apeglm.

Bioinformatic pathway analysis. GSEA using the Hallmark, Gene Ontology biological processes, and KEGG databases was conducted with the fgsea package v1.22.0 [68]. Heatmaps were generated using normalised counts and *Z*-scores scaled using the Complex Heatmaps package v2.12.1 [69]. Volcano plots were generated using SRPLOT software, using a $\log_2$ fold-change of specific genes in the dataset. A gene was considered significantly differentially expressed if it demonstrated an adjusted p-value < 0.05 and $\log_2$ FC > 1.5. Sequence data are available from the GEO database under accession number GSE248341.

Statistical analysis

Two thousand to two thousand and five hundred islets per pancreas are routinely isolated from mice, and statistical power analysis was carried out for each in vitro 19 methods based on data generated in similar experiments. The following sample sizes are required for 90% power with a confidence level of 5% to detect significant differences between treatment groups: (i) Static incubations experiments from isolated islets require 8 replicates while reformed islets require 4 replicates (ii) Reformed Islet apoptosis assays require 10 replicates, while isolated islets require 6 replicates.

Statistical analysis and graphical representation of the data were performed using GraphPad Prism software (version 9.5.1; GraphPad Software, La Jolla, CA, USA). Statistical comparisons were performed using one- or two-way ANOVA, followed by Šídák's or Dunnett's multiple comparison tests. All results are expressed as the mean ± SEM. Statistical significance was defined as a p value < 0.05 and is denoted as stars in the graphs ($*p < 0.05$; $**p < 0.01$; $***p < 0.001$; $****p < 0.0001$) in all figures, unless otherwise stated.

DATA AVAILABILITY

All RNA sequencing data are deposited in the Gene Expression Omnibus database under accession code GSE248341. The experimental data sets generated and/or analysed during the current study are available from the corresponding author upon reasonable request.

REFERENCES

1. Khan MAB, Hashim MJ, King JK, Govender RD, Mustafa H, Al Kaabi J. Epidemiology of type 2 diabetes - global burden of disease and forecasted trends. J Epidemiol Glob Health. 2020;10:107–11.
2. Lin X, Xu Y, Pan X, Xu J, Ding Y, Sun X, et al. Global, regional, and national burden and trend of diabetes in 195 countries and territories: an analysis from 1990 to 2025. Sci Rep. 2020;10:14790.
3. R Paul Robertson M. Type 2 diabetes mellitus: prevalence and risk factors. UpToDate. 2023. https://www.uptodate.com/contents/type-2-diabetes-mellitus-prevalence-and-riskfactors#:~:text=Other%20national%20databases%2C%20such%20as,undiagnosed%2C%20and%2095%20percent%20of
4. Segerstolpe A, Palasantza A, Eliasson P, Andersson EM, Andreasson AC, Sun X, et al. Single-cell transcriptome profiling of human pancreatic islets in health and type 2 diabetes. Cell Metab. 2016;24:593–607.
5. Carter JD, Dula SB, Corbin KL, Wu R, Nunemaker CS. A practical guide to rodent islet isolation and assessment. Biol Proced Online. 2009;11:3–31.
6. Marchini A, Ciulla MG, Antonioli B, Agnoli A, Bovio U, Visnoviz V, et al. Long-term cultures of human pancreatic islets in self-assembling peptides hydrogels. Front Bioeng Biotechnol. 2023;11:1105157.
7. Skelin M, Rupnik M, Cencic A. Pancreatic beta cell lines and their applications in diabetes mellitus research. ALTEX. 2010;27:105–13.
8. Kaido T, Yebra M, Cirulli V, Rhodes C, Diaferia G, Montgomery AM. Impact of defined matrix interactions on insulin production by cultured human beta-cells: effect on insulin content, secretion, and gene transcription. Diabetes. 2006;55:2723–9.
9. Phelps EA, Cianciaruso C, Santo-Domingo J, Pasquier M, Galliverti G, Piemonti L, et al. Advances in pancreatic islet monolayer culture on glass surfaces enable super-resolution microscopy and insights into beta cell ciliogenesis and proliferation. Sci Rep. 2017;7:45961.
10. Weinberg N, Ouziel-Yahalom L, Knoller S, Efrat S, Dor Y. Lineage tracing evidence for in vitro dedifferentiation but rare proliferation of mouse pancreatic beta-cells. Diabetes. 2007;56:1299–304.
11. Lin JY, Cheng J, Du YQ, Pan W, Zhang Z, Wang J, et al. In vitro expansion of pancreatic islet clusters facilitated by hormones and chemicals. Cell Discov. 2020;6:20.
12. Riopel M, Li J, Fellows GF, Goodyer CG, Wang R. Ultrastructural and immunohistochemical analysis of the 8-20 week human fetal pancreas. Islets. 2014;6:e982949.
13. Liu B, Ruz-Maldonado I, Toczyska K, Olaniru OE, Zariwala MG, Hopkins D, et al. The selective serotonin reuptake inhibitor fluoxetine has direct effects on beta cells, promoting insulin secretion and increasing beta-cell mass. Diabetes Obes Metab. 2022;24:2038–50.
14. Liberzon A, Subramanian A, Pinchback R, Thorvaldsdottir H, Tamayo P, Mesirov JP. Molecular signatures database (MSigDB) 3.0. Bioinformatics. 2011;27:1739–40.

15. Steiner DJ, Kim A, Miller K, Hara M. Pancreatic islet plasticity: interspecies comparison of islet architecture and composition. Islets. 2010;2:135–45.
16. Zirpel H, Roep BO. Islet-resident dendritic cells and macrophages in type 1 diabetes: in search of bigfoot's print. Front Endocrinol. 2021;12:666795.
17. Cosentino C, Regazzi R. Crosstalk between macrophages and pancreatic beta-cells in islet development, homeostasis and disease. Int J Mol Sci. 2021;22:1765.
18. Thai LM, O'Reilly L, Reibe-Pal S, Sue N, Holliday H, Small L. et al. Beta-cell function is regulated by metabolic and epigenetic programming of islet-associated macrophages, involving Axl, Mertk, and TGFbeta receptor signaling. iScience. 2023;26:106477.
19. Xu G, Stoffers DA, Habener JF, Bonner-Weir S. Exendin-4 stimulates both beta-cell replication and neogenesis, resulting in increased beta-cell mass and improved glucose tolerance in diabetic rats. Diabetes. 1999;48:2270–6.
20. Benninger RK, Piston DW. Cellular communication and heterogeneity in pancreatic islet insulin secretion dynamics. Trends Endocrinol Metab. 2014;25:399–406.
21. Henquin JC, Dufrane D, Kerr-Conte J, Nenquin M. Dynamics of glucose-induced insulin secretion in normal human islets. Am J Physiol Endocrinol Metab. 2015;309:E640–50.
22. Liberzon A, Birger C, Thorvaldsdottir H, Ghandi M, Mesirov JP, Tamayo P. The molecular signatures database (MSigDB) hallmark gene set collection. Cell Syst. 2015;1:417–25.
23. Nurmagambetova A, Mustyatsa V, Saidova A, Vorobjev I. Morphological and cytoskeleton changes in cells after EMT. SciRep. 2023;13:22164. https://doi.org/10.1038/s41598-023-48279-y.
24. Moreno-Amador JL, Tellez N, Marin S, Aloy-Reverte C, Semino C, Nacher M, et al. Epithelial to mesenchymal transition in human endocrine islet cells. PLoS ONE. 2018;13:e0191104.
25. Hayashi Y, Kuroda T, Kishimoto H, Wang C, Iwama A, Kimura K. Downregulation of rRNA transcription triggers cell differentiation. PLoS ONE. 2014;9:e98586.
26. Taneera J, Storm P, Groop L. Downregulation of type II diabetes mellitus and maturity onset diabetes of young pathways in human pancreatic islets from hyperglycemic donors. J Diabetes Res. 2014;2014:237535.
27. Nishimura W, Iwasa H, Tumurkhuu M. Role of the Transcription Factor MAFA in the Maintenance of Pancreatic β-Cells. Int J Mol Sci. 2022;23:4478. https://doi.org/10.3390/ijms23094478.
28. Randeria SN, Thomson GJA, Nell TA, Roberts T, Pretorius E. Inflammatory cytokines in type 2 diabetes mellitus as facilitators of hypercoagulation and abnormal clot formation. Cardiovasc Diabetol. 2019;18:72.
29. Tsalamandris S, Antonopoulos AS, Oikonomou E, Papamikroulis GA, Vogiatzi G, Papaioannou S, et al. The role of inflammation in diabetes: current concepts and future perspectives. Eur Cardiol. 2019;14:50–9.
30. de Candia P, Prattichizzo F, Garavelli S, De Rosa V, Galgani M, Di Rella F, et al. Type 2 Diabetes: how much of an autoimmune disease? Front Endocrinol. 2019;10:451.
31. Feuerer M, Shen Y, Littman DR, Benoist C, Mathis D. How punctual ablation of regulatory T cells unleashes an autoimmune lesion within the pancreatic islets. Immunity. 2009;31:654–64.
32. Rukstalis JM, Habener JF. Snail2, a mediator of epithelial-mesenchymal transitions, expressed in progenitor cells of the developing endocrine pancreas. Gene Expr Patterns. 2007;7:471–9.
33. Gershengorn MC, Hardikar AA, Wei C, Geras-Raaka E, Marcus-Samuels B, Raaka BM. Epithelial-to-mesenchymal transition generates proliferative human islet precursor cells. Science. 2004;306:2261–4.
34. Atkinson MA, von Herrath M, Powers AC, Clare-Salzler M. Current concepts on the pathogenesis of type 1 diabetes–considerations for attempts to prevent and reverse the disease. Diabetes Care. 2015;38:979–88.
35. Ehses JA, Perren A, Eppler E, Ribaux P, Pospisilik JA, Maor-Cahn R, et al. Increased number of islet-associated macrophages in type 2 diabetes. Diabetes. 2007;56:2356–70.
36. van Gurp L, Fodoulian L, Oropeza D, Furuyama K, Bru-Tari E, Vu AN, et al. Generation of human islet cell type-specific identity genesets. Nat Commun. 2022;13:2020.
37. Brissova M, Fowler MJ, Nicholson WE, Chu A, Hirshberg B, Harlan DM, et al. Assessment of human pancreatic islet architecture and composition by laser scanning confocal microscopy. J Histochem Cytochem. 2005;53:1087–97.
38. Lorza-Gil E, Kaiser G, Rexen Ulven E, König GM, Gerst F, Oquendo MB, et al. FFA2-, but not FFA3-agonists inhibit GSIS of human pseudoislets: a comparative study with mouse islets and rat INS-1E cells. Sci Rep. 2020;10:16497.
39. Bowe JE, Chander A, Liu B, Persaud SJ, Jones PM. The permissive effects of glucose on receptor-operated potentiation of insulin secretion from mouse islets: a role for ERK1/2 activation and cytoskeletal remodelling. Diabetologia. 2013;56:783–91.
40. Fusco J, Xiao X, Prasadan K, Sheng Q, Chen C, Ming YC, et al. GLP-1/Exendin-4 induces beta-cell proliferation via the epidermal growth factor receptor. Sci Rep. 2017;7:9100.
41. Wang C, Chen X, Ding X, He Y, Gu C, Zhou L. Exendin-4 promotes beta cell proliferation via PI3k/Akt signalling pathway. Cell Physiol Biochem. 2015;35:2223–32.
42. Matsushima H, Kuroki T, Adachi T, Kitasato A, Ono S, Tanaka T, et al. Human fibroblast sheet promotes human pancreatic islet survival and function in vitro. Cell Transplant. 2016;25:1525–37.
43. Perez-Basterrechea M, Esteban MM, Alvarez-Viejo M, Fontanil T, Cal S, Sanchez Pitiot M, et al. Fibroblasts accelerate islet revascularization and improve long-term graft survival in a mouse model of subcutaneous islet transplantation. PLoS ONE. 2017;12:e0180695.
44. Nilsson J, Fardoos R, Hansen L, Lovkvist H, Pietras K, Holmberg D, et al. Recruited fibroblasts reconstitute the peri-islet membrane: a longitudinal imaging study of human islet grafting and revascularisation. Diabetologia. 2020;63:137–48.
45. Homo-Delarche F, Drexhage HA. Immune cells, pancreas development, regeneration and type 1 diabetes. Trends Immunol. 2004;25:222–9.
46. Denroche HC, Miard S, Salle-Lefort S, Picard F, Verchere CB. T cells accumulate in non-diabetic islets during ageing. Immun Ageing. 2021;18:8.
47. Suk K, Kim S, Kim YH, Kim KA, Chang I, Yagita H, et al. IFN-gamma/TNF-alpha synergism as the final effector in autoimmune diabetes: a key role for STAT1/IFN regulatory factor-1 pathway in pancreatic beta cell death. J Immunol. 2001;166:4481–9.
48. Boni-Schnetzler M, Meier DT. Islet inflammation in type 2 diabetes. Semin Immunopathol. 2019;41:501–13.
49. Banu S, Sur D. Role of macrophage in type 2 diabetes mellitus: macrophage polarization a new paradigm for treatment of type 2 diabetes mellitus. Endocr Metab Immune Disord Drug Targets. 2023;23:2–11.
50. Rooijen Van N, Sanders A. Liposome mediated depletion of macrophages: mechanism of action, preparation of liposomes and applications. J Immunol Methods. 1994;174:83–93.
51. Lee KU, Amano K, Yoon JW. Evidence for initial involvement of macrophage in development of insulitis in NOD mice. Diabetes. 1988;37:989–91.
52. Jun HS, Santamaria P, Lim HW, Zhang ML, Yoon JW. Absolute requirement of macrophages for the development and activation of beta-cell cytotoxic CD8+ T-cells in T-cell receptor transgenic NOD mice. Diabetes. 1999;48:34–42.
53. Jun HS, Yoon CS, Zbytnuik L, van Rooijen N, Yoon JW. The role of macrophages in T cell-mediated autoimmune diabetes in nonobese diabetic mice. J Exp Med. 1999;189:347–58.
54. Carrero JA, McCarthy DP, Ferris ST, Wan X, Hu H, Zinselmeyer BH, et al. Resident macrophages of pancreatic islets have a seminal role in the initiation of autoimmune diabetes of NOD mice. Proc Natl Acad Sci USA. 2017;114:E10418–E27.
55. Nikolic T, Geutskens SB, van Rooijen N, Drexhage HA, Leenen PJ. Dendritic cells and macrophages are essential for the retention of lymphocytes in (peri)-insulitis of the nonobese diabetic mouse: a phagocyte depletion study. Lab Investig. 2005;85:487–501.
56. Ye Z, Chen L, Yang Z, Li Q, Huang Y, He M, et al. Metabolic effects of fluoxetine in adults with type 2 diabetes mellitus: a meta-analysis of randomized placebo-controlled trials. PLoS ONE. 2011;6:e21551.
57. Ghaeli P, Shahsavand E, Mesbahi M, Kamkar MZ, Sadeghi M, Dashti-Khavidaki S. Comparing the effects of 8-week treatment with fluoxetine and imipramine on fasting blood glucose of patients with major depressive disorder. J Clin Psychopharmacol. 2004;24:386–8.
58. Zhu S, Bai Q, Li L, Xu T. Drug repositioning in drug discovery of T2DM and repositioning potential of antidiabetic agents. Comput Struct Biotechnol J. 2022;20:2839–47.
59. Mali P, Yang L, Esvelt KM, Aach J, Guell M, DiCarlo JE, et al. RNA-guided human genome engineering via Cas9. Science. 2013;339:823–6.
60. Cong L, Ran FA, Cox D, Lin S, Barretto R, Habib N, et al. Multiplex genome engineering using CRISPR/Cas systems. Science. 2013;339:819–23.
61. Hering BJ, Clarke WR, Bridges ND, Eggerman TL, Alejandro R, Bellin MD, et al. Phase 3 trial of transplantation of human islets in type 1 diabetes complicated by severe hypoglycemia. Diabetes Care. 2016;39:1230–40.
62. Brewer GJ, Torricelli JR, Evege EK, Price PJ. Optimized survival of hippocampal neurons in B27-supplemented neurobasal, a new serum-free medium combination. J Neurosci Res. 1993;35:567–76.
63. Gey GO, Gey MK The Maintenance of Human Normal Cells and Tumor Cells in Continuous Culture: I. 30Preliminary Report: Cultivation of Mesoblastic Tumors and Normal Tissue and Notes on Methods of Cultivation. Am J Cancer. 1936;27:45–76.
64. Li P, Hao Z, Wu J, Ma C, Xu Y, Li J, et al. Comparative proteomic analysis of polarized human THP-1 and mouse RAW264.7 macrophages. Front Immunol. 2021;12:700009.
65. Justus CR, Leffler N, Ruiz-Echevarria M, Yang LV. In vitro cell migration and invasion assays. J Vis Exp. 2014:51046. https://doi.org/10.3791/51046.
66. Taciak B, Bialasek M, Braniewska A, Sas Z, Sawicka P, Kiraga L, et al. Evaluation of phenotypic and functional stability of RAW 264.7 cell line through serial passages. PLoS ONE. 2018;13:e0198943.

67. Love MI, Huber W, Anders S. Moderated estimation of fold change and dispersion for RNA-seq data with DESeq2. Genome Biol. 2014;15:550.
68. Korotkevich G. Fast gene set enrichment analysis. BioRxiv. 2019. https://doi.org/10.1101/060012.
69. Gu Z, Eils R, Schlesner M. Complex heatmaps reveal patterns and correlations in multidimensional genomic data. Bioinformatics. 2016;32:2847–9.

ACKNOWLEDGEMENTS

We thank the families of donors and the Cell Therapy Unit in the NIHR/Wellcome King's Clinical Research Facility for making human islets available for research and Dr. Tzu-Wen Hong, KCL for generating the IMARIS image.

AUTHOR CONTRIBUTIONS

NH and GAB designed and managed the studies. NH, KWT, MEW, MJ, MZ, YL, JAP, SJP, TJP, and GAB contributed to the writing and editing of the manuscript. NH, KWT, MZ, YL, and ZS carried out all the islet studies. JAP isolated and provided the murine T cells. MEW, MJ, GAB, and TJP analysed the sequencing data.

FUNDING

This work was supported by Juvenile Diabetes Research Foundation (JDRF) grant awarded to Dr Bewick (3-SRA-2022-1162-S-B) and Medical Research Council Doctoral Training Programme studentship for Ms Margot Jacobs (ST12201).

COMPETING INTERESTS

The authors declare no competing interests.

ETHICS APPROVAL AND CONSENT TO PARTICIPATE

All animal experiments were approved by the King's College London Animal Welfare and Ethical Review Board and were performed in accordance with the British Home Office Animal Scientific Procedures Act (1986). All human islets were retrieved from non-diabetic, heart-beating, and brain-dead donors and isolated by cold collagenase digestion [23, 61] in accordance with relevant guidelines and regulations with appropriate ethical approval from the King's College London Human Islet Research Tissue Bank (KCL HI-RTB; 20/SW/0074). An assent form was completed by a relative of the pancreas donor for all the islets used in the study.

ADDITIONAL INFORMATION

Supplementary information The online version contains supplementary material available at https://doi.org/10.1038/s41420-024-02234-6.

Correspondence and requests for materials should be addressed to G. A. Bewick.

Reprints and permission information is available at http://www.nature.com/reprints

Publisher's note Springer Nature remains neutral with regard to jurisdictional claims in published maps and institutional affiliations.